

Metalized T graphene: A reversible hydrogen storage material at room temperature

Xiao-Juan Ye, Chun-Sheng Liu, Wei Zhong, Zhi Zeng, and You-Wei Du

Citation: *Journal of Applied Physics* **116**, 114304 (2014); doi: 10.1063/1.4895778

View online: <http://dx.doi.org/10.1063/1.4895778>

View Table of Contents: <http://scitation.aip.org/content/aip/journal/jap/116/11?ver=pdfcov>

Published by the [AIP Publishing](#)

Articles you may be interested in

[Curvature and ionization-induced reversible hydrogen storage in metalized hexagonal B36](#)

J. Chem. Phys. **141**, 194306 (2014); 10.1063/1.4902062

[Polylithiated \(OLi₂\) functionalized graphane as a potential hydrogen storage material](#)

Appl. Phys. Lett. **101**, 243902 (2012); 10.1063/1.4772208

[Li-doped B₂C graphene as potential hydrogen storage medium](#)

Appl. Phys. Lett. **98**, 173101 (2011); 10.1063/1.3583465

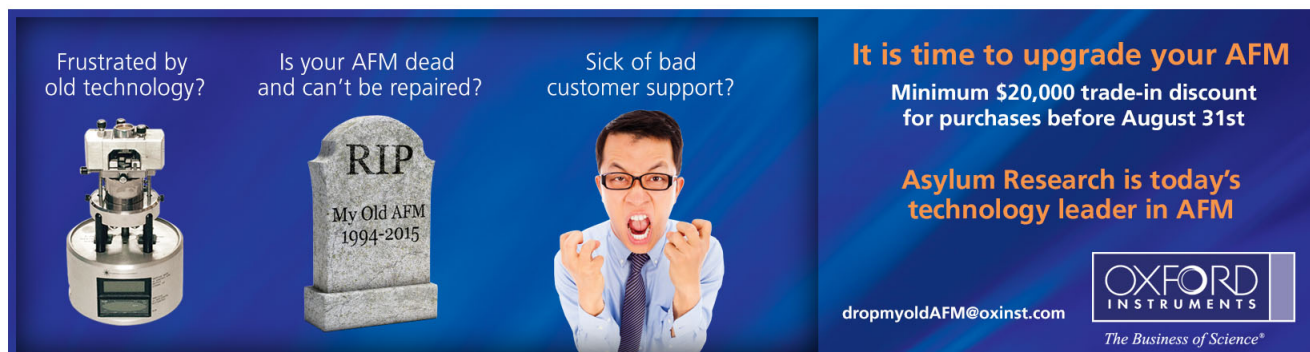
[Al doped graphene: A promising material for hydrogen storage at room temperature](#)

J. Appl. Phys. **105**, 074307 (2009); 10.1063/1.3103327

[Hydrogen storage in alkali-metal-decorated organic molecules](#)

Appl. Phys. Lett. **93**, 063107 (2008); 10.1063/1.2971201

Frustrated by old technology? Is your AFM dead and can't be repaired? Sick of bad customer support?



It is time to upgrade your AFM
Minimum \$20,000 trade-in discount for purchases before August 31st

Asylum Research is today's technology leader in AFM

dropmyoldAFM@oxinst.com

OXFORD INSTRUMENTS
The Business of Science®

Metalized *T* graphene: A reversible hydrogen storage material at room temperature

Xiao-Juan Ye,¹ Chun-Sheng Liu,^{2,a)} Wei Zhong,^{1,a)} Zhi Zeng,³ and You-Wei Du¹

¹Nanjing National Laboratory of Microstructures, Nanjing University, Nanjing 210093, People's Republic of China

²Key Laboratory of Radio Frequency and Micro-Nano Electronics of Jiangsu Province, Nanjing University of Posts and Telecommunications, Nanjing 210023, People's Republic of China

³Key Laboratory of Materials Physics, Institute of Solid State Physics, Chinese Academy of Sciences, Hefei 230031, People's Republic of China

(Received 28 July 2014; accepted 3 September 2014; published online 16 September 2014)

Lithium (Li)-decorated graphene is a promising hydrogen storage medium due to its high capacity. However, homogeneous mono-layer coating graphene with lithium atoms is metastable and the lithium atoms would cluster on the surface, resulting in the poor reversibility. Using van der Waals-corrected density functional theory, we demonstrated that lithium atoms can be homogeneously dispersed on *T* graphene due to a nonuniform charge distribution in *T* graphene and strong hybridizations between the C-2*p* and Li-2*p* orbitals. Thus, Li atoms are not likely to form clusters, indicating a good reversible hydrogen storage. Both the polarization mechanism and the orbital hybridizations contribute to the adsorption of hydrogen molecules (storage capacity of 7.7 wt. %) with an optimal adsorption energy of 0.19 eV/H₂. The adsorption/desorption of H₂ at ambient temperature and pressure is also discussed. Our results can serve as a guide in the design of new hydrogen storage materials based on non-hexagonal graphenes. © 2014 AIP Publishing LLC.

[<http://dx.doi.org/10.1063/1.4895778>]

I. INTRODUCTION

Hydrogen has been considered as a clean alternative energy carrier because of its efficiency, abundance, and environmental friendliness. Materials suitable for hydrogen storage must meet the requirements of high gravimetric/volumetric storage density, fast kinetics, favorable thermodynamics, and good reversibility.¹

Recently, many studies have been performed on carbon-based nanostructures due to their light weight and interesting properties.^{2–8} However, hydrogen molecules bind weakly to pristine carbon materials via van der Waals interactions. Therefore, metal atoms coated the carbon surfaces have been presented to improve storage performance. For example, coating carbon nanostructures with early transition-metals (TM) can enhance the hydrogen adsorption energies via the Kubas interaction.^{3–5} After releasing hydrogen, however, the isolated TM atoms would cluster together easily, which is unfavorable for reversible hydrogen storage.⁷ In addition, excessive charge transfers from TM to the antibonding σ state of H₂ frequently lead to the first hydrogen dissociation. On the other hand, alkali metals such as Li can coat uniformly due to the cohesive energy of Li being substantially smaller than that of TMs (~ 4 eV).⁸ However, it is not always true for Li to bind strongly to all carbon nanostructures. Especially, the binding energies of Li on ethylene (0.69 eV/Li)⁵ and graphene (1.10 eV/Li)⁹ are smaller than the cohesive energy of bulk Li, namely, 1.63 eV/Li. The clustering of metal atoms may come from the uniform charge distribution on pristine

graphene with a regular hexagonal symmetry. Therefore, it is necessary to enhance the Li binding on these carbon materials, since the Li atom is lightweight which can help to achieve a higher gravimetric density of hydrogen.

In the search for the reversible hydrogen storage media, we now turn to the graphene allotrope without hexagonal symmetry owing to its nonuniform charge distribution which can enhance the metal bonding and improve the hydrogen storage performance. Very recently, a novel *T* graphene (a two-dimensional carbon allotrope with tetrahedrals) has been predicted.¹⁰ However, Kim *et al.*¹¹ demonstrated that the fully relaxed buckled *T* graphene cannot be distinguishable with the planar one, indicating that the buckled *T* graphene will only be stable at high temperatures. These results inspired us to consider a series of calculations to explore whether hydrogen storage performance in Li-decorated *T* graphene can be significantly improved compared with that in Li-decorated graphene. To address this issue, we investigated the Li-decorated *T* graphene and found that it is a good reversible hydrogen storage material.

II. COMPUTATIONAL METHODS

The first-principles density-functional theory (DFT) calculations were carried out using the linear combination of atomic orbital and spin-unrestricted method implemented in DMol³ package.¹² The generalized gradient approximation (GGA)^{13,14} in the Perdew-Burke-Ernzerhof (PBE) functional form¹⁵ together with an all-electron double numerical basis set with polarization function (the DNP basis set) were chosen for the DFT calculation. We performed van der Waals calculations based on the Tkatchenko and Scheffler (DFT-

^{a)}Authors to whom correspondence should be addressed. Electronic addresses: csliu@njupt.edu.cn and wzhang@nju.edu.cn.

TS) approaches.¹⁶ The real-space global cutoff radius was set to be 4.10 Å. In the case of *T* graphene, we chose 2×2 (namely, C₁₆) and 4×4 (namely, C₆₄) supercells. The inter-layer distance was set to be 25 Å, which is enough to minimize the artificial interlayer interactions. The Brillouin zones were sampled *k*-points with 0.02 \AA^{-1} spacing using Monkhorst-Pack scheme.¹⁷ For geometric optimization, the forces on all atoms were optimized to be less than 0.02 eV \AA^{-1} .

III. RESULTS AND DISCUSSIONS

We first examine the adsorption of Li atoms on the *T* graphene. This is modeled by one Li atom adsorbed on each (2×2) cell of *T* graphene (namely, C:Li = 16:1). After fully relaxation, the most energetically favorable adsorption site for the Li atom is the hollow site above the center of octagon (see Fig. 1(a)). The nearest Li-Li distance is about 6.9 Å which is larger than that in Li-doped graphene (4.92 Å) and Li-doped B₂C sheet (5.12 Å), indicating that each Li atom can adsorb the hydrogen molecules. The binding energy (2.34 eV) of Li on C₁₆ is much higher than the cohesive energy of bulk Li (1.63 eV/Li). Due to the repulsive interaction between positively charged Li atoms, the binding energy of LiC₁₆ is smaller than that of LiC₆₄ (4×4) cell. It is known that the diffusion of metal atoms on the substrate might lead

to clustering,⁷ which will limit the hydrogen storage. As shown in Fig. 1(b), our model is energetically favorable due to the repulsion between Li atoms, which can effectively hinder the mobility of Li on the substrate. Therefore, one individual Li atom bound to the *T* graphene will reside stable at the original site.

To understand the nature of the binding of Li on *T* graphene, analysis of the electronic properties is essential. Figure 1(c) illustrates the partial density of states (PDOS) of LiC₁₆, where Li 2*p* orbitals participate in the bonding. The attached Li first donates the 2*s* electrons to the *T* graphene (see Fig. 1(d)), leading to partially filled lowest unoccupied molecule orbitals (LUMO). Meanwhile, the empty Li 2*p* orbitals split under the strong ligand field generated by the *T* graphene. Then the *T* graphene back-donates some electrons to the low-lying Li 2*p* orbitals, resulting in strong *p-p* and *s-p* hybridizations between Li and *T* graphene in the energy range from -10 to -2 eV. Note that *T* graphene and graphene generate different ligand fields because of their distinct symmetries. The bonding nature of Li adsorbed on graphene is mostly mediated by the ionic interactions.⁹ This bonding mechanism has also been observed in the case of Li binding onto the boron-doped graphene⁶ and the B₈₀.¹⁸

We now enter the next phase of our calculation, namely, to study the adsorption of H₂ molecules on Li-decorated *T* graphene. Figures 2(a) and 2(b) present the optimized

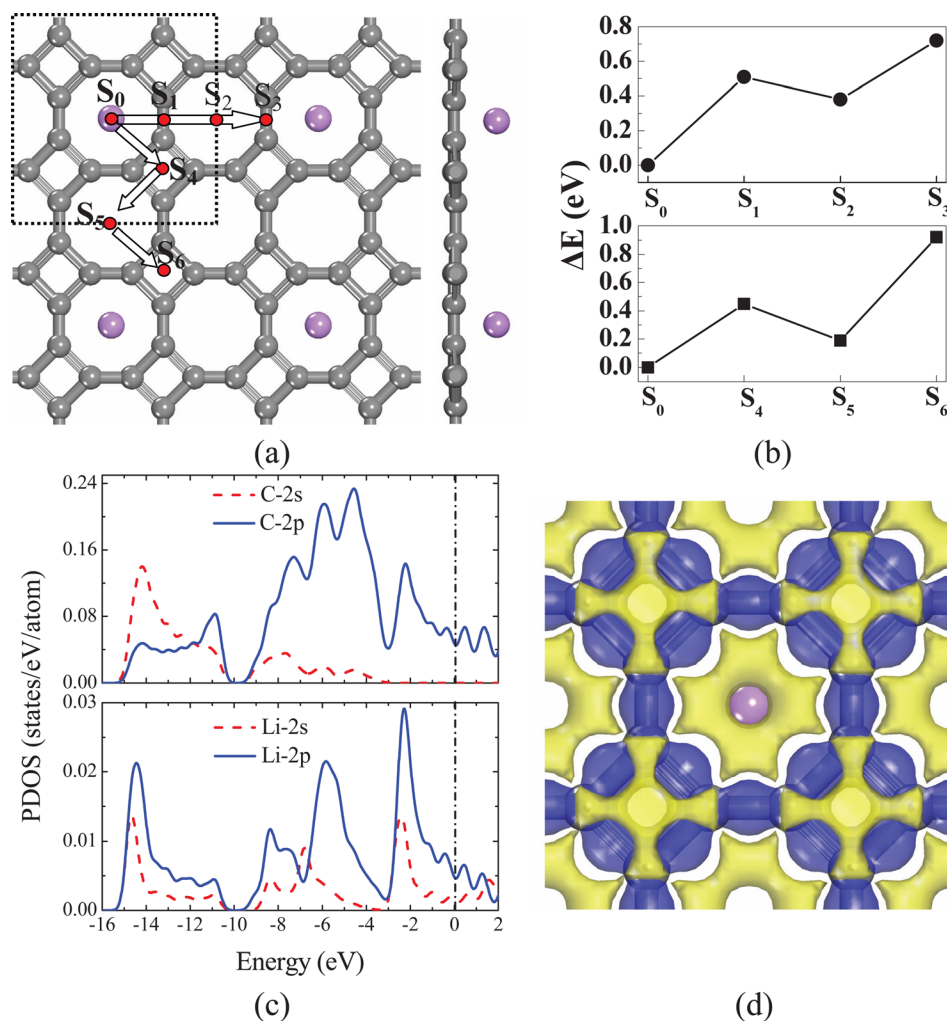


FIG. 1. (a) Top view and side view of optimized geometry for 2×2 cell of LiC₁₆. (b) The variation in total energy as the top-left Li atom moves through the position S₁, S₂, and S₃ indicated in (a). As this Li atom moves in the direction, its *z* coordinate is optimized, whereas the remaining three Li atoms are fully relaxed. Beyond the positions S₁, S₂, and S₃ of this Li atom, the Coulomb repulsion will push the top-right Li atom to maintain a distance with the top-left Li atom. Similarly, the variation in total energy as the top-left Li atom moves in the other direction beyond the positions S₄, S₅, and S₆ is shown in the (b). (c) The PDOS of C and Li atoms corresponding to the system in (a). The Fermi level is set to be zero. The panel (d) shows the deformation electron densities of LiC₁₆ (molecular charge densities minus atomic charge densities). The deformed density marked in blue corresponds to the region that contains excess electrons, while that marked in yellow indicates electron loss.) The isovalue equals 0.1 e/\AA^3 .

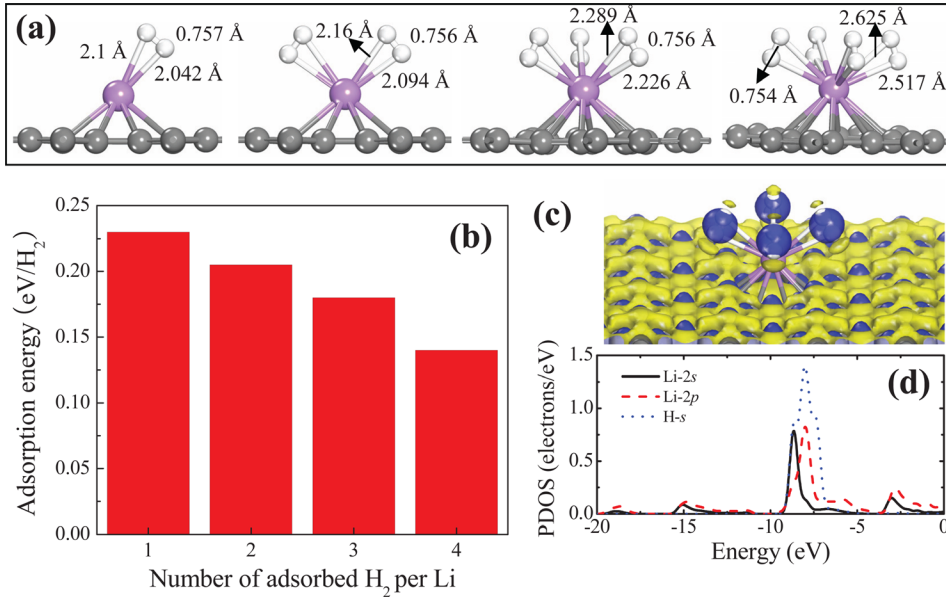


FIG. 2. (a) The optimized configurations of $\text{LiC}_{16}-(\text{H}_2)_n = 1-4$. Large, medium, and small balls represent Li, C, and H atoms, respectively. (b) The variation in the calculated E_a of $\text{LiC}_{16}-(\text{H}_2)_n = 1-4$. The panel (c) presents a plot of charge density difference with an isovalue of $0.03 \text{ e}/\text{\AA}^3$ for $(\text{H}_2)_4\text{-LiC}_{16}$. (d) PDOS of Li and H_2 in $(\text{H}_2)_4\text{-LiC}_{16}$.

geometries and average hydrogen adsorption energies (E_a), where $E_a = [E(\text{Li} + T \text{ graphene}) + n \times E(\text{H}_2) - E(n\text{H}_2 + \text{Li} + T \text{ graphene})]/n$. In contrast with previous studies on Li-decorated graphene (0.09 eV),¹⁹ the adsorption energy for the first hydrogen molecule on Li-decorated T graphene is calculated to be as high as 0.23 eV , and the H-H bond length is slightly elongated from 0.749 \AA to 0.757 \AA . Up to four H_2 molecules in succession can be bound to the Li atom with a distance of $\sim 2.63 \text{ \AA}$, as shown in Fig. 2(a). As the number of H_2 molecules increases, the binding energy of the H_2 molecules decreases slightly due to the steric interaction between adsorbed H_2 molecules. This adsorption is still much stronger than previously reported H_2 adsorption ($-0.075 \text{ eV}/\text{H}_2$) on Li-C₆₀ systems based on the GGA functional.⁸ Recently, unphysical overbinding by DFT calculations in the Ca-H₂ system has been revealed with the correct description of hybridization involving the d orbital on Ca being implicated.²⁰ However, this is not expected to be problematic in the Li-H₂ system, due to the absence of d orbitals on the Li atom. Previous MP2 calculations have indeed also shown favorable adsorption of H_2 in Li-H₂ system.²¹

There are two main factors responsible for the H_2 binding. The first is polarization. Because of the charge transfer between Li and T graphene, Li atoms are positively charged, which polarizes the H_2 molecule. In the Fig. 2(c), we plot the isosurface of differential charge density for Li-decorated T graphene in the presence of four adsorbed hydrogen molecules. The charge depletion and accumulation at both sides of the H_2 molecule clearly indicate that hydrogen molecules are strongly polarized by the highly charged Li^+ ion. The second is orbital interactions. Through the PDOS analysis (see Fig. 2(d)), we find that the peak of Li $2p$ orbitals hybridizes with the H s orbitals, resulting in the electron transfer between H_2 σ orbitals and Li $2p$ orbitals. The consequences of the orbital interactions are as well reflected in the charge variations of the Li. The effective charge of the Li atom decreases as the number of adsorbed hydrogen molecules per Li atom increases from 1 to 4 (see Table I). For example, the Hirshfeld charge of the Li atom in the $4\text{H}_2\text{-C}_{16}\text{Li}$ complex has been reduced to $0.20 e$.

To estimate the usable capacity of hydrogen at ambient conditions, we considered the thermodynamics of adsorption of H_2 molecules on the Li + T graphene complex. The occupation number of H_2 molecules as a function of the pressure and temperature from the grand canonical partition function is as follows:²²

$$f = kT \frac{\partial \ln Z}{\partial \mu} = \frac{\sum_{l=0}^{\infty} l g_l e^{l(\mu - \varepsilon_l/kT)}}{\sum_{l=0}^{\infty} g_l e^{l(\mu - \varepsilon_l/kT)}}, \quad (1)$$

where Z is the grand partition function, μ is the chemical potential of H_2 in the gas phase at given pressure p and temperature T , k is the Boltzmann constant, ε_l is the adsorption energy per H_2 molecule when the number of adsorbed molecules is l , g_l is the multiplicity (degeneracy) of the configuration for a given l . Here we set the degeneracy factor g_l to be 1, since it was turned out to give a minor correction to the result. Figure 3(a) shows the occupation number f as a function of p and T for H_2 adsorbed on LiC₁₆. When the pressure increases from 1 atm to 50 atm, the release temperature will be shifted to around 350 K, which is suitable for the on-board storage of hydrogen. To obtain the usable amount of hydrogen, we propose to use the adsorption condition of 50 atm and 200 K, and the desorption condition of 1 atm and 350 K. The usable numbers of hydrogen molecules per Li is defined to be $f(p = 50 \text{ atm}, T = 200 \text{ K})$ minus $f(p = 1 \text{ atm}, T = 350 \text{ K})$. In the case of Li-decorated T graphene, 2.2 H_2 molecules remain used when p and T change from the

TABLE I. The Hirshfeld and Mulliken net charge of the Li atom in C_{16}Li , $\text{C}_{16}\text{Li-H}_2$, $\text{C}_{16}\text{Li-2H}_2$, $\text{C}_{16}\text{Li-3H}_2$, and $\text{C}_{16}\text{Li-4H}_2$.

Structure	Hirshfeld charge (e)	Mulliken charge (e)
C_{16}Li	+0.40	+0.46
$\text{C}_{16}\text{Li-H}_2$	+0.36	+0.40
$\text{C}_{16}\text{Li-2H}_2$	+0.33	+0.37
$\text{C}_{16}\text{Li-3H}_2$	+0.30	+0.35
$\text{C}_{16}\text{Li-4H}_2$	+0.20	+0.24

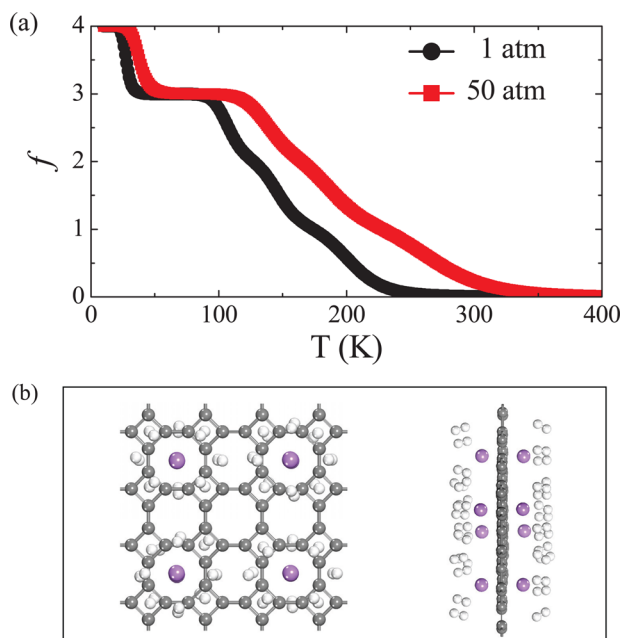


FIG. 3. (a) The number of adsorbed H_2 on LiC_{16} under thermal equilibrium as a function of temperature at 1 atm and 50 atm. (b) Top view and side view of the optimized geometry for 32 H_2 molecules adsorbed on $8Li-C_{64}$. Large, medium, and small balls represent Li, C, and H atoms, respectively.

adsorption condition to the desorption condition. This is ascribed to the fact that the binding energy of the fourth adsorbed H_2 molecule is relatively small [see Fig. 2(b)].

Lithium atoms can form a dense coverage on T graphene with a Li-Li distance of 6.90 Å and are expected to resist clustering due to electrostatic interaction between the cationic adsorbed Li atoms. To further test the stability of the isolated Li_8C_{64} complex, we carried out molecular dynamics simulations at room temperature ($T=300$ K) with a time step of 1 fs and massive generalized Gaussian moments thermostat with Nosé chain length of 2 and a Yoshida parameter of 3.²³ After running 5000 steps, these four configurations are still kept and each Li bind on its site stably.

The maximum number of adsorbed Li atoms in (4×4) cell of T graphene is four for each side. We examine the case of four adsorbed hydrogen molecules around each Li atom since this ratio retains the higher adsorption energies. Figure 3(b) shows the optimized geometries for 32 H_2 molecules adsorbed on $8Li-C_{64}$, with the average binding energy around 0.19 eV. The H_2 gravimetric density corresponding to the $(H_2)_{32}-Li_8C_{64}$ complex is 7.7 wt. %, which is much higher than the limit (6 wt. %) set for the feasible hydrogen. Although the high H_2 storage capacity was also achieved in the Li-decorated graphene, the preferable clustering of Li atoms on graphene significantly reduces the weight percentage of hydrogen storage.

IV. CONCLUSIONS

In summary, our first-principles studies have demonstrated Li as a potential coating metal element for functionalizing T graphene into a feasible hydrogen storage medium. The Li atoms remain isolated due to the strong binding between Li and T graphene which is attributed to an intriguing charge transfer mechanism involving the empty Li $2p$ levels. The adsorption of hydrogen molecules on Li-decorated T graphene is significantly enhanced with up to a 7.7 wt. % hydrogen storage capacity potentially feasible. We anticipate that the theoretical results here will provide a useful reference for designing new hydrogen storage media based on 2D carbon allotropes without hexagonal symmetry.

ACKNOWLEDGMENTS

This work was supported by the National Natural Science Foundation (Grant Nos. 11174132 and 11104278) and the National Key Project for Basic Research (Grant Nos. 2011CB922102 and 2012CB932304).

- ¹See the special issue Toward a Hydrogen Economy, by R. Coontz and B. Hanson, *Science* **305**, 957 (2004).
- ²J. Zhou, Q. Wang, Q. Sun, P. Jena, and X. S. Chen, *Proc. Natl. Acad. Sci. U.S.A.* **107**, 2801 (2010); P. Jena, *J. Phys. Chem. Lett.* **2**, 206 (2011); Q. Wang, Q. Sun, P. Jena, and Y. Kawazoe, *ACS Nano* **3**, 621 (2009).
- ³T. Yildirim and S. Ciraci, *Phys. Rev. Lett.* **94**, 175501 (2005).
- ⁴Y. F. Zhao, Y. H. Kim, A. C. Dillon, M. J. Heben, and S. B. Zhang, *Phys. Rev. Lett.* **94**, 155504 (2005).
- ⁵E. Durgun, S. Ciraci, W. Zhou, and T. Yildirim, *Phys. Rev. Lett.* **97**, 226102 (2006).
- ⁶C. S. Liu and Z. Zeng, *Phys. Rev. B* **79**, 245419 (2009).
- ⁷Q. Sun, Q. Wang, P. Jena, and Y. Kawazoe, *J. Am. Chem. Soc.* **127**, 14582 (2005).
- ⁸Q. Sun, P. Jena, Q. Wang, and M. Marquez, *J. Am. Chem. Soc.* **128**, 9741 (2006).
- ⁹C. Ataca, E. Aktürk, S. Ciraci, and H. Ustunel, *Appl. Phys. Lett.* **93**, 043123 (2008).
- ¹⁰Y. Liu, G. Wang, Q. Huang, L. Guo, and X. Chen, *Phys. Rev. Lett.* **108**, 225505 (2012).
- ¹¹B. G. Kim, J. Y. Jo, and H. S. Sim, *Phys. Rev. Lett.* **110**, 029601 (2013).
- ¹²B. Delley, *J. Chem. Phys.* **92**, 508 (1990).
- ¹³W. Kohn and L. J. Sham, *Phys. Rev.* **140**, A1133 (1965).
- ¹⁴M. Schluter and L. J. Sham, *Phys. Today* **35**(2), 36 (1982).
- ¹⁵J. P. Perdew, K. Burke, and M. Ernzerhof, *Phys. Rev. Lett.* **77**, 3865 (1996).
- ¹⁶A. Tkatchenko and M. Scheffler, *Phys. Rev. Lett.* **102**, 073005 (2009).
- ¹⁷H. Monkhorst and J. Pack, *Phys. Rev. B* **13**, 5188 (1976).
- ¹⁸Y. C. Li, G. Zhou, J. Li, B. L. Gu, and W. H. Duan, *J. Phys. Chem. C* **112**, 19268 (2008).
- ¹⁹A. Du, Z. Zhu, and S. Smith, *J. Am. Chem. Soc.* **132**, 2876 (2010).
- ²⁰J. Cha, S. Lim, C. H. Choi, M. H. Cha, and N. Park, *Phys. Rev. Lett.* **103**, 216102 (2009).
- ²¹J. G. Vitillo, A. Damin, A. Zecchina, and G. Ricchiardi, *J. Chem. Phys.* **122**, 114311 (2005).
- ²²H. Lee, W. I. Choi, and J. Ihm, *Phys. Rev. Lett.* **97**, 056104 (2006).
- ²³B. Delley, *Comput. Mater. Sci.* **17**, 122 (2000).